IAA-AAS-DyCoSS1-05-10

EARTH-MOON LIBRATION STATIONKEEPING: THEORY, MODELING, AND OPERATIONS

David C. Folta*, Mark Woodard *

&

Tom Pavlak[§], Amanda Haapala[§], Kathleen Howell[‡]

Abstract

Collinear Earth-Moon libration points have emerged as locations with immediate applications. These libration point orbits are inherently unstable and must be controlled at a rapid frequency which constrains operations and maneuver locations. Stationkeeping is challenging due to short time scales of divergence, effects of large orbital eccentricity of the secondary body, and third-body perturbations. Using the Acceleration Reconnection and Turbulence and Electrodynamics of the Moon's Interaction with the Sun (ARTEMIS) mission orbit as our platform (hypothesis), we contrast and compare promising stationkeeping strategies including Optimal Continuation and Mode Analysis that achieved consistent and reasonable operational stationkeeping costs. Background on the fundamental structure and the dynamical models to achieve these demonstrated results are discussed along with their mathematical development.

INTRODUCTION

Earth-Moon collinear libration points have emerged as locations with immediate applications. To fully understand the selection of Earth-Moon (EM) libration orbit orientations and amplitudes as well as the inherent problems of stationkeeping, this paper offers the following: the originating theory of EM libration orbit evolution, the use of Poincaré maps to define and select orbit characteristics, the required modeling of the libration point orbits, the computation of the stability of the Earth-Moon orbits, and includes the in-flight stationkeeping strategies, observations, and experiences. Operational considerations are also included. Using the Acceleration Reconnection and Turbulence and Electrodynamics of the Moon's Interaction with the Sun (ARTEMIS) mission as our platform (hypothesis), we contrast and compare operationally demonstrated and validated strategies: (i) the Optimal Continuation Strategy (OCS) which employs various numerical methods to determine maneuver locations while minimizing costs, and (ii) an implementation of Floquet modes and manifold information calculated from navigation states. Both these approaches develop optimal maneuver locations and delta-V (Δv) directions. These orbits are inherently unstable and must be controlled at a rapid frequency that constrains operations and maneuver locations. Stationkeeping of these orbits is challenging because of short time scales of divergence, the effects of large orbital eccentricity of the secondary, and solar gravitational and radiation pressure perturbations. To this end, the stationkeeping strategies presented minimize fuel while operationally providing for quality navigation tracking and maneuver planning scenarios. Results using operational data are demonstrated in Poincaré maps and in the implementation of these stationkeeping strategies.

CONSIDERATIONS OF THE EARTH-MOON SYSTEM

With any model difference in energy from truth, a spacecraft will depart from the desired EM L_1 or EM L_2 orbit along an unstable manifold, either towards the Moon or in an escape direction. These escape directions can be towards the Earth or towards Sun-Earth regions (transferring onto the stable manifold in the

* Aerospace Engineer, NASA Goddard Space Flight Center, Greenbelt, Maryland 20771.

§ Graduate Student, Purdue University, School of Aeronautics and Astronautics, West Lafayette, Indiana 47907-2045.

‡ Hsu Lo Professor of Aeronautical and Astronautical Engineering, Purdue University, School of Aeronautics and Astronautics, West Lafayette, Indiana 47907-2045. Fellow AAS; Associate Fellow AIAA.

Sun-Earth system). The Δv required to affect these changes is exceedingly small, where even a mis-modeling of accelerations from solar radiation pressure or a natural perturbation will result in these escape trajectories. Therefore, the Earth-Moon system must be modeled as a true four-body problem, including the Sun's gravity as an important third-body acceleration. Along with the lunar eccentricity and solar radiation pressure accelerations, there are also operational aspects of any mission based on the spacecraft design flight constraints. Stationkeeping then becomes a task in high fidelity modeling for accurate trajectory predictions along with maneuver implementation that also matches environmental conditions.

To determine the orbit stability (instability), one can perform a Mode Analysis using the eigenstructure (eigenvectors and eigenvalues) of the libration point orbit. By computing the 6 eigenvalues, λ_i, of the navigation State Transition Matrix (STM) one can determine $|\lambda_i| < 1 \rightarrow$ stable eigenvalue(s) or $|\lambda_i| > 1 \rightarrow$ unstable eigenvalue(s). Once the mode information is generated, one can predict the stability of the orbit and compare the planned maneuver directions with stable/unstable eigenvector information. Our operational results indicate that consistent and reasonable stationkeeping costs can be achieved with accurate models and maneuver strategies with the selection dependent upon spacecraft and operational limitations and constraints. To continue the orbit downstream and maintain the path in the vicinity of the libration point, one can selectively choose target goals around the libration orbit. For the method applied directly to ARTEMIS, these goals were directly related to the energy (velocity) at the *x*-*z* plane crossing to wrap the orbit in the proper direction, tentatively inward (unstable manifold) towards the libration point. A Poincaré map of Earth-Moon orbits is presented to demonstrate the structure of these orbits with respect to theoretical and operational motion. Cost comparisons in terms of executed maneuvers are presented between the different approaches. With unique operational constraints, accomplishment of the maintenance goals with the minimum cost in terms of propellant is usually the highest priority.

ARTEMIS Background

For the discussion of the applications in this paper, one should understand the fundamentals of the ARTEMIS mission which we use as our basis of investigation. ARTEMIS is the first mission flown to and continuously maintained in orbit about both collinear Earth-Moon libration points, EM L_1 and EM L_2. [1-5] The ARTEMIS mission transferred two of five Time History of Events and Macroscale Interactions during Substorms (THEMIS) spacecraft from their outer-most elliptical Earth orbits and, with lunar gravity assists, re-directed them to both EM L_1 and EM L_2 via transfer trajectories that exploit the Sun-Earth multi-body dynamical environment. Two identical ARTEMIS spacecraft, named P1 and P2, entered Earth-Moon libration point orbits in 2010 on August 25th and October 22nd, respectively. Once the Earth-Moon libration point orbits were achieved, they were maintained for eleven months, with the P1 spacecraft orbiting EM L_2 and P2 orbiting EM L_1. During this stationkeeping phase, the P1 spacecraft was transferred from EM L_2 to EM L_1. From these EM libration orbits, both spacecraft were inserted into elliptical lunar orbits in 2011on June 27th and July 17th, respectively.

The ARTEMIS libration orbits of the P1 spacecraft around the EM L_2 / L_1 and the P2 spacecraft around EM L_1 appear in Figures 1 and 2, respectively. There were no size or orientation requirements on these orbits other than to minimize the insertion and orbital maintenance requirements and to permit a transfer into a lunar orbit with low inclination. Both ARTEMIS spacecraft had limited combined deterministic and statistical stationkeeping Δv budgets of ~15 m/s and ~12 m/s for P1 and P2, respectively. This Δv budget included the libration point orbit stationkeeping, the transfers between libration orbits, and the transfer into lunar orbit. The P1 and P2 L_1 *y*-amplitudes were approximately 60,000 km with the P1 L_2 *y*-amplitude near 68,000 km. The overall amplitudes are determined from the use of a ballistic Sun-Earth to Earth-Moon transfer insertion. Consequently, at the end of the multi-body transfer, the final lunar libration point orbit was influenced heavily by the Moon since the transfer orbit passes relatively close to the Moon at each negative *x*-*z* plane crossing with respect to the L_2 libration point. The libration orbit dimensions appear in Table 1.

Table 1. ARTEMIS Libration Orbit Dimensions

	ARTEMIS P1 @ L1	ARTEMIS P1 @ L2	ARTEMIS P2 @ L1
Maximum *x*-Amplitude (km)	**23656**	**32686**	**30742**
Maximum *y*-Amplitude (km)	**58816**	**63520**	**67710**
Maximum *z*-Amplitude (km)	**2387**	**35198**	**4680**
Minimum *z*-Amplitude (km)	**181**	**n/a**	**246**
Period (days), average of 10 subsequent *x*-*z* plane axis crossings	**13.51**	**15.47**	**14.19**

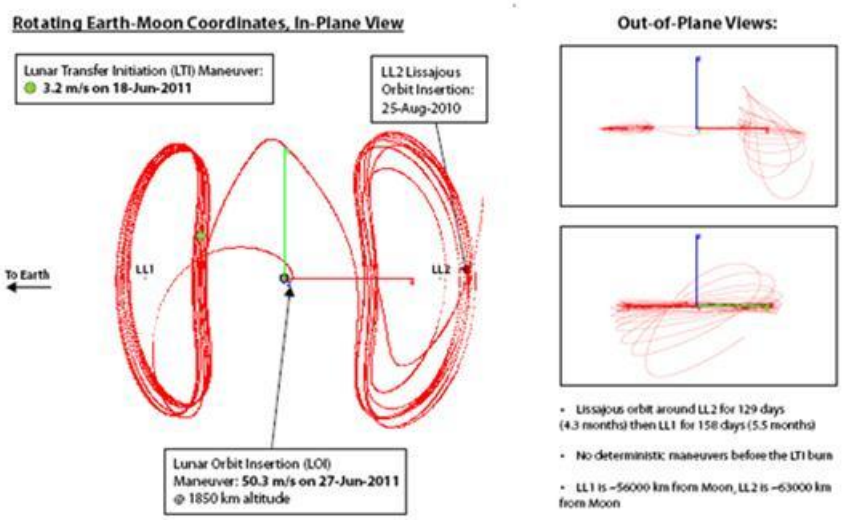

Figure 1. ARTEMIS P1 Libration Orbit

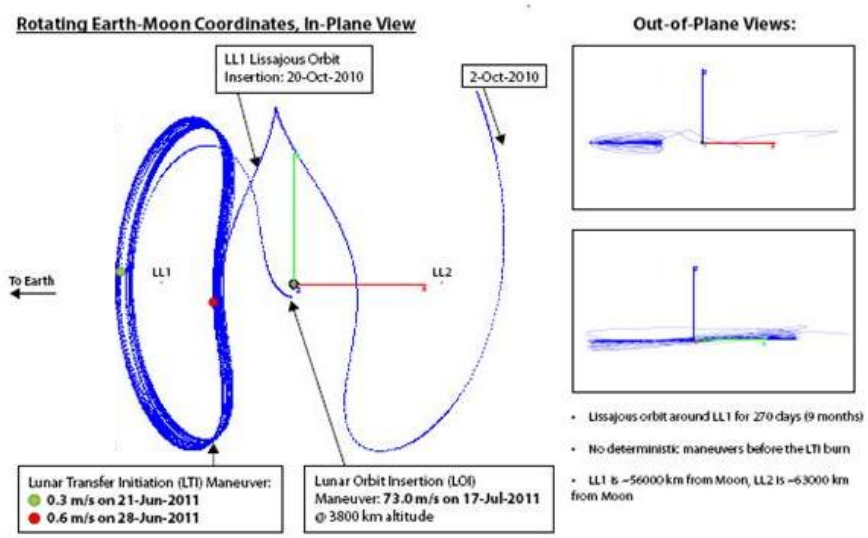

Figure 2. ARTEMIS P2 Libration Orbit

THEORETICAL OVERVIEW AND ORBIT GENERATION

While the final design for the ARTEMIS mission required high fidelity modeling, analysis of the libration orbits from the perspective of the Circular Restricted Three-Body (CR3B) problem yields much insight into the governing dynamics. In the CR3B model,[6] the motion of a spacecraft, assumed massless, is governed by two massive primary bodies, the Earth and the Moon, each represented as a point mass. The orbits of the primary bodies are assumed circular relative to the system barycenter. A barycentered rotating frame is defined such that the rotating $\hat{x}$-axis is directed from the Earth to the Moon, the $\hat{z}$-axis is parallel to the direction of the angular velocity of the primary system, and the $\hat{y}$-axis completes the dextral orthonormal triad. Defining the mass parameter, $\mu = \dfrac{m_1}{m_1 + m_2}$, the non-dimensional distances to the primaries are $\bar{r}_1 = \left[-\mu, 0, 0\right]^T$ and $\bar{r}_2 = \left[1-\mu, 0, 0\right]^T$. The position vectors defined in terms of rotating coordinates are written as $\bar{r} = \left[x, y, z\right]^T$, $\bar{r}_{13} = \left[x-\mu, y, z\right]^T$, and $\bar{r}_{23} = \left[x-1+\mu, y, z\right]^T$. The first-order, non-dimensional, vector equation of motion is

$$\dot{\bar{x}} = \bar{f}\left(\bar{x}\right) \quad \text{where} \tag{1}$$

$$\bar{f} = \left[\dot{x}, \dot{y}, \dot{z}, 2\dot{y} + U_x, -2\dot{x} + U_x, U_z\right]^T \tag{2}$$

The pseudo-potential, U, is defined $U\left(x, y, z\right) = \dfrac{1-\mu}{r_{13}} + \dfrac{\mu}{r_{23}} + \dfrac{1}{2}\left(x^2 + y^2\right)$, and quantities U_x, U_y, U_z represent partial derivatives of U with respect to rotating position coordinates. The single, scalar integral of the motion, known as the Jacobi constant, *C*, is represented as $C = 2U\left(x, y, z\right) - v^2$, where $v = \left(\dot{x}^2 + \dot{y}^2 + \dot{z}^2\right)^{1/2}$.

Five equilibrium points exist, including three collinear libration points, L_1, L_2, and L_3, that lie along the $\hat{x}$-axis, and two equilateral points L_4 and L_5. Linear analysis of the collinear points [6-9] reveals that they possess a topological structure of the type saddle×center×center, thus, asymptotic flow to and away from the libration points is possible via the stable and unstable manifolds, respectively; periodic and quasi-periodic libration orbits exist within the center manifold. Selecting states such that they exist within the center manifold yields the following variational equations, centered at the libration point, describing libration orbits: $\delta x\left(t\right) = A_x \cos\left(\nu t + \phi\right), \delta y\left(t\right) = A_y \cos\left(\nu t + \phi\right), \delta z\left(t\right) = A_z \cos\left(\omega t + \psi\right)$ where $i\nu, i\omega$ represent the eigenvalues associated with the planar and out-of-plane center manifolds, respectively, angles ϕ, ψ represent phase angles, and amplitudes A_x, A_y are related by a proportionality constant. Because $\nu \neq \omega$, these equations describe quasi-periodic motion in the vicinity of the collinear points. Selecting $A_z = 0$ yields the planar, periodic Lyapunov orbits, while, choosing $A_x = A_y = 0$, the periodic vertical orbits emerge.

An example of a quasi-periodic orbit appears in black in Figure 3a; note that the orbit is linearized about the L_1 point, but is plotted in a Moon-centered view. The δz evolution appears in Figure 3b, and illustrates the constant amplitude, A_z. By adjusting the phase angles ϕ, ψ, it is possible to enter the libration orbit in different locations. As an example, the red segments in Figures 3a-3b represent shifts in angles ψ and ϕ that allow for entry into the orbit at a different δz location. The variational equations exist within the framework of a linear analysis, however periodic and quasi-periodic orbits also exist in the full non-linear model, described by equations (1-2).[10] Several methods exist for computing periodic and quasi-periodic libration orbits with the inclusion of non-linear effects.[11-15] A quasi-periodic orbit in the CR3B problem is depicted in Figure 4a; the corresponding *z*-amplitude evolution appears in Figure 4b. Clearly, the A_z amplitude

is no longer constant, but cycles between high and low *z*-amplitude modes. By shifting the entry phasing, it is possible to enter the quasi-periodic orbit at a different location and alter the *z*-amplitude mode. The red highlighted regions of Figure 4 demonstrate how the entry location in the orbit can be shifted to enter the orbit during the nearly planar mode.

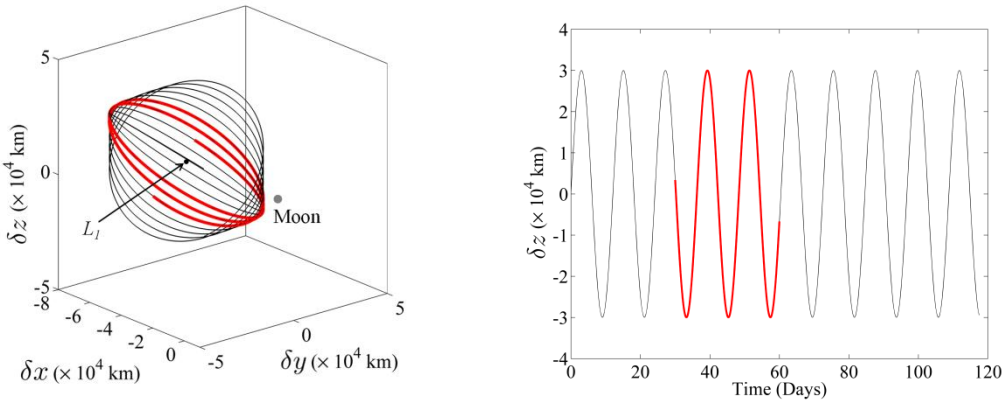

a) Quasi-periodic orbit in linear model, Moon-centered view

b) δz -amplitude evolution over time

Figure 3. Quasi-Periodic Orbit in the Linear Model, with corresponding δz -Amplitude Evolution.

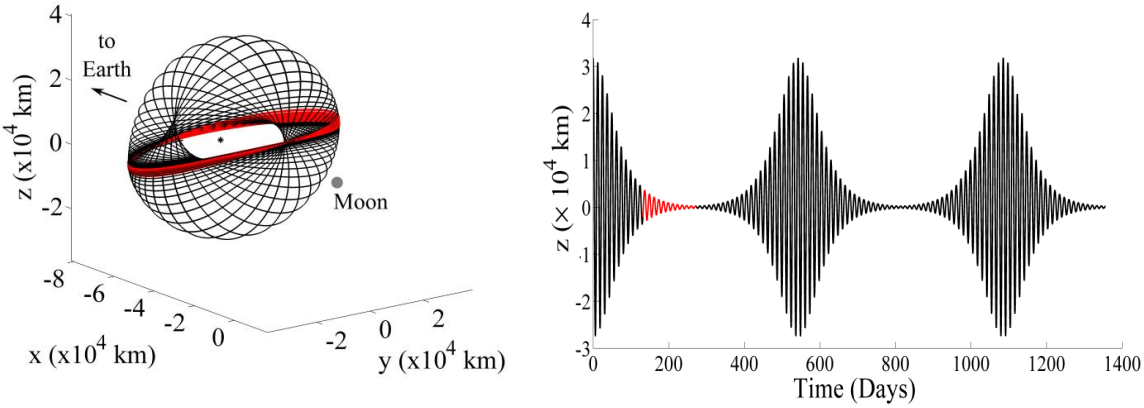

a) Quasi-periodic orbit in CR3B model, Moon centered view

b) *z*-amplitude evolution over time

Figure 4. Quasi-Periodic Orbit in the CR3B Model Cycles through High and Low *z*-Amplitude Modes.

Poincaré Maps

To obtain a more complete picture of the available libration point orbit solutions, it is useful to employ Poincaré maps. Through the use of a Poincaré map, an *n*-dimensional continuous-time system is reduced to a discrete-time system of (*n*-1)-dimensions. By additionally constraining the Jacobi constant, C , the problem is reduced to (*n*-2)-dimensions, and the map is represented in 4-D. To generate a Poincaré map, a surface-of-section, Σ, is defined such that Σ is transversal to the flow, e.g., $\Sigma = \{\overline{x} : z = 0\}$ represents the surface-of-section corresponding to crossings of the *x*-*y* plane. For the CR3B problem, trajectories are integrated using

equations (1-2), and crossings of Σ are displayed on the map. Consider the map in Figure 6, reproduced to resemble maps demonstrated by Gómez et al.,[16] as well as Kolemen et al.[14]

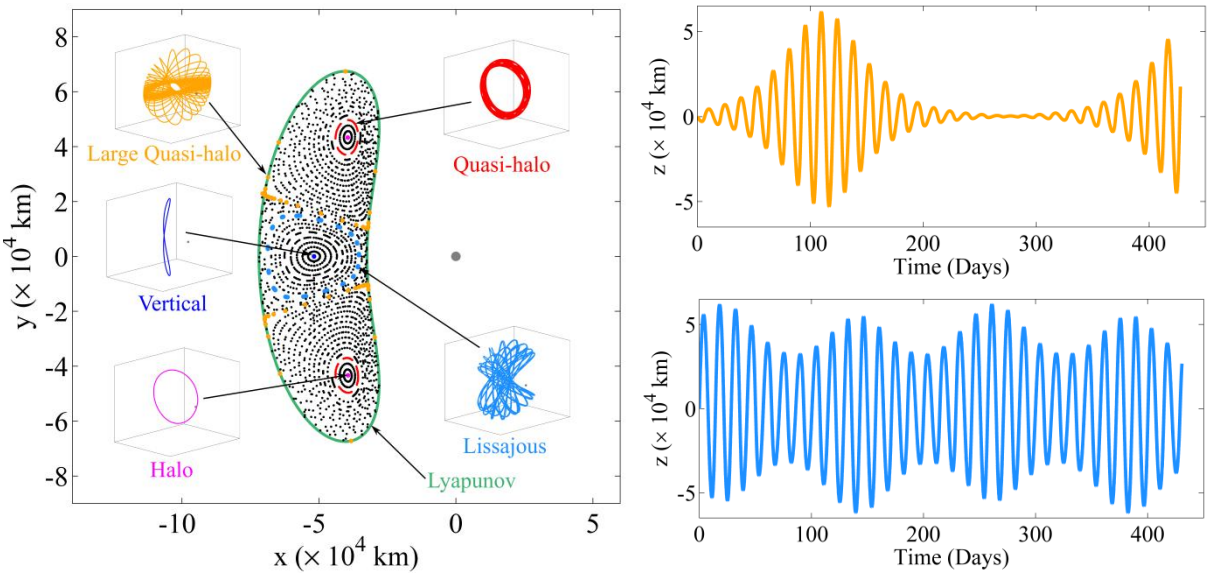

a) Poincaré map corresponding to crossings of the *x*-*y* plane, with sample orbits featured.

b) *z*-amplitude evolution of selected orbits

Figure 5. Poincaré Map Depicting Periodic and Quasi-Periodic Libration Point Orbit Structures in the Vicinity of L_1 in the Earth-Moon System for C = 3.080.

For the selected value of *C*, several periodic orbits exist, including a planar Lyapunov orbit (green), a vertical orbit (dark blue), and the northern and southern halo orbits. The halo orbits share the same crossings of the map, and the northern halo is featured in magenta in Figure 5a. Surrounding the vertical orbits are quasi-periodic orbits, often denoted Lissajous orbits, which exist within the center subspace of the vertical. A sample Lissajous is featured in cyan. Similarly, the quasi-halo orbits lie in the center manifold of the central halo orbit. Examples of small and large northern quasi-halo orbits appear in red and orange, respectively. These distinct regions of quasi-periodic behavior are explored in detail by Barden and Howell.[17] The *z*-amplitude evolutions corresponding to the large quasi-halo and Lissajous orbits featured in Figure 5a appear in Figure 5b. The periodic halo and vertical orbits possess constant A_z amplitudes, whereas the quasi-periodic orbits exhibit oscillating values of A_z. The crossings of the Lissajous orbits are contained within the central region of the map; therefore, these orbits do not possess the nearly planar modes demonstrated in Figure 4. The quasi-halo orbit crossings occur in the upper and lower regions of the map, and, thus, both high and low *z*-amplitude modes are facilitated by selection of a quasi-halo orbit.

ARTEMIS Poincaré Maps

To gain insight into the types of orbits employed in ARTEMIS, Poincaré maps are generated to display the orbit structures associated with each libration point orbit energy level. Both L_1 and L_2 quasi-periodic libration orbits were incorporated in the ARTEMIS mission. In the original mission design, the P1 spacecraft spends an interval of ~131 days in orbit about the L_2 point, followed by a transfer to an orbit about L_1 for ~85 days. The P2 spacecraft remains in orbit about L_1 for approximately 154 days. The ARTEMIS trajectories are designed with higher-fidelity ephemeris modeling, and the true paths possess discontinuities in the form of small Δvs. Thus, to analyze the libration orbits using maps, it is desirable to compute orbits qualitatively similar to those of the ARTEMIS mission in the CR3B model. To transition to the CR3B problem, the ARTEMIS

libration orbits are sampled by distributing nodes along the orbit paths, and are then re-converged in the CR3B model using a differential corrections process to ensure full-state continuity. For each of the converged trajectories, the Jacobi value, *C*, is evaluated and maps are generated that correspond to the appropriate libration point and the specified energy level. Because the ARTEMIS orbits and the converged CR3B libration orbits appear qualitatively the same, the results from the discussion of the CR3B orbits apply to the actual ARTEMIS orbits as well. Maps for the P1 L_2, P1 L_1, and P2 L_1 libration orbits appear in Figures 6-8, respectively.

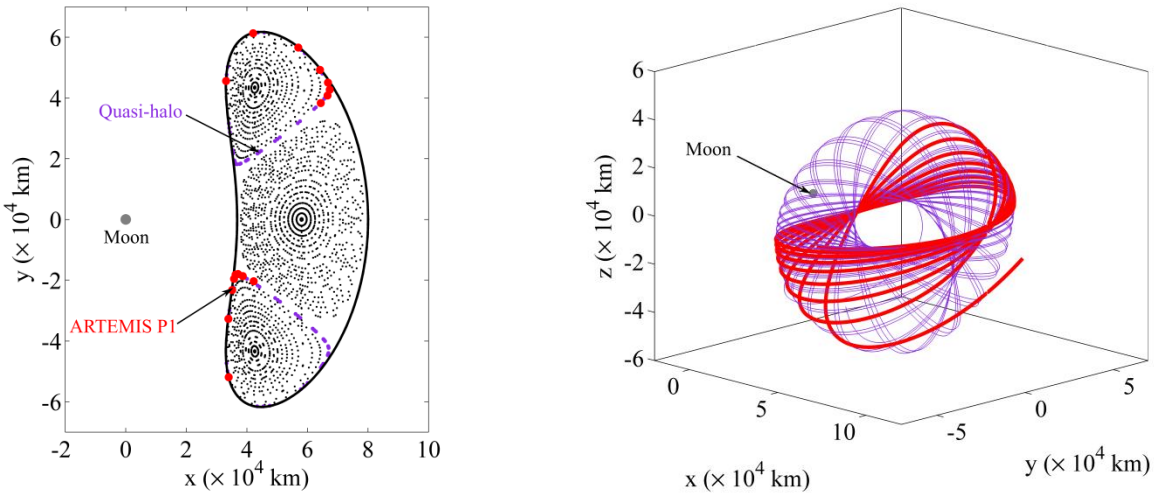

a) Map corresponding to P1 L_2 orbit

b) P1 L_2 orbit (red) with a southern quasi-halo of similar size (purple)

Figure 6. Poincaré Map associated with the P1 L_2 ARTEMIS Orbit (*C* = 3.105)

Each of the three ARTEMIS libration orbits possesses crossings (in red) of the map that lie in the quasi-halo region. In Figures 6b, 7b, and 8b, quasi-halo orbits with map crossings that lie close to each of the ARTEMIS libration orbit crossings appear with the CR3B converged ARTEMIS trajectories plotted in red to demonstrate the long-term evolution of these libration orbits. The quasi-halo orbit crossings are highlighted in color on the maps and lie close to the ARTEMIS spacecraft crossings.

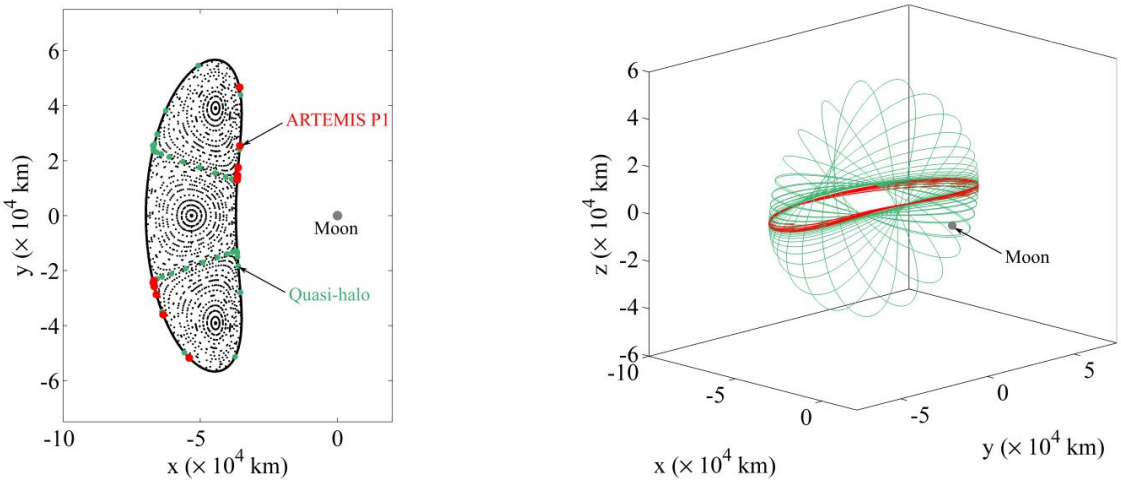

a) Map corresponding to P2 L_1 orbit

b) P1 L_1 orbit (red) with a southern quasi-halo of similar size (green

Figure 7. Poincaré Map associated with the P1 L_1 ARTEMIS Orbit (*C* = 3.105)

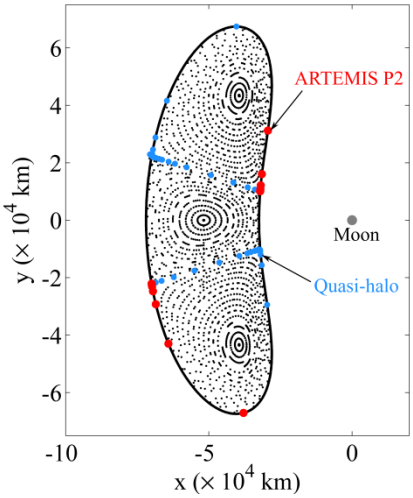

a) Map corresponding to P2 L_1 orbit

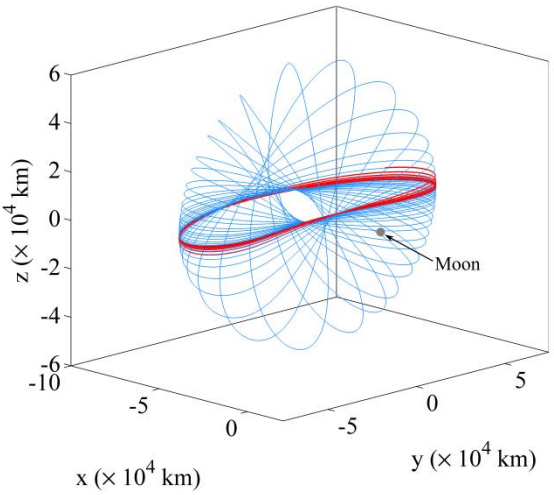

a) P2 L_1 orbit (red) with a northern quasi-halo of similar size (blue)

Figure 8. Poincaré Map associated with the P2 L_1 ARTEMIS Orbit (C = 3.080).

ENVIRONMENT MODELING

The Environment

It is important to utilize adequate environmental models in order to progress from a CR3B dynamical formulation to an operational environment and to support the stationkeeping strategies provided in this paper. As noted previously, in the Earth-Moon system, lunar eccentricity and solar gravity significantly influence libration point orbit stability and these effects should be modeled very accurately.

Full Ephemeris Models

For ARTEMIS, and as recommended for all operational missions, one should use a full ephemeris model (DE421 file) along with third-body perturbations, including solar radiation pressure acceleration based on the spacecraft mass and cross-sectional area (e.g. a simplified spacecraft cannon ball model or one that reflects a higher fidelity one), a potential model for the Earth with degree and order eight is recommended. The numerical integration of the equation of motion for recent operational plans was based on a variable step Runge-Kutta 8/9 or Dormand-Prince 8/9 integrator. The libration point locations were also calculated instantaneously at the same integration interval. To compute maneuver requirements in terms of Δv, different strategies involve various numerical methods: traditional Differential Correction (DC) targeting with central or forward differencing, or optimization using the VF13AD algorithm from the Harwell library and Sequential Quadratic Programming (SQP) Optimization. For the DC, equality constraints (velocity targets) are incorporated, while for the optimization scheme, nonlinear equality and inequality constraints are employed. Software that can be employed to meet spacecraft constraints and orbit goals for stationkeeping effort includes GSFC's General Mission Analysis Tool (GMAT) (open source s/w) and AGI's STK/Astrogator. Once the environment has been properly modeled, the next step is maintaining the orbit.

EARTH-MOON LIBRATION STATIONKEEPING STRATEGIES

A variety of stationkeeping strategies have previously been investigated for applications in the Sun-Earth system and near the Earth-Moon libration points. To be useful, a stationkeeping strategy must satisfy several conditions: use full ephemeris with high-fidelity models, provide globally optimized solutions, and apply to Earth-Moon orbital requirements at L_1 or L_2 and any transfer between them. Several approaches should

not be operationally employed for various reasons, e.g., because a reference orbit is required which is not necessarily available nor desired (or not correctly modeled); the strategy is based on the CR3B model which may not meet true perturbation effects; the stationkeeping process is based on linear control, which may be acceptable if the orbit is pre-designed using high fidelity models, but may require frequent maneuvers; or because a proposed approach cannot accommodate spacecraft constraints. Numerous references in the literature offer discussion of stability and control for vehicles at both collinear and triangular libration point locations. Hoffman[18] and Farquhar[19] both provide analysis and discussion of stability and control in the Earth-Moon collinear L_1 and L_2 locations, respectively, within the context of classical control theory or linear approximations; Scheeres offers a statistical analysis approach.[20] Howell and Keeter[21] address the use of selected maneuvers to eliminate the unstable modes associated with a reference orbit; Gomez et al.[22] developed and applied the approach specifically to translunar libration point orbits. Marchand and Howell[23] discuss stability including the eigenstructures near the Sun-Earth locations. Folta and Vaughn[24] present an analysis of stationkeeping options and transfers between the Earth-Moon locations, and the use of numerical models that include discrete linear quadratic regulators and differential correctors. Pavlak and Howell[25] have demonstrated maintenance using dynamical systems modes. Lastly, Folta et al.[1-5] provided both a review of all pertinent stationkeeping methods for stationkeeping in Earth-Moon libration orbits with intent of application to ARTEMIS, and the operational results of the first EM L_1 an EM L_2 mission, its transfer to these orbits, the intra-transfer from EM L_2 to EM L_1, and the final transfer to lunar orbits.

OPTIMAL CONTINUATION STRATEGY (OCS)

From research by the authors and the imposed operational constraints, the Optimal Continuation Strategy (OCS) was chosen and was verified by Mode Analysis using operational navigation data.[1] As summarized in Table 2, this strategy balances the orbit by meeting goals at crossing events several revolutions downstream, thereby ensuring a continuous orbit without constraining the near-term evolution or the reliance on specific orbit size or orientation specifications. This also provided for the inclusion of several lunar orbits.

This method uses goals in the form of energy achieved, velocities, or time at any location along the orbit. For example, a goal might be defined in terms of the *x*-axis velocity component at the *x*-*z* plane crossing. While a DC scheme with Δv components was used to initialize the analysis in our pre-flight research, for operations we switched to an SQP optimizer that uses Δv magnitude, Δv azimuth (a spacecraft constraint), and maneuver epoch as controls. The orbit is continued over several revolutions by checking the conditions at each successive goal. This allows perturbations and the lunar orbit eccentricity to be modeled over multiple revolutions. Targeting is implemented with parameters assigned at the *x*-*z* plane crossing such that the orbit is continued and another revolution is achieved. The VF13AD and SQP optimizers were used to minimize the stationkeeping Δv by optimizing the direction of the Δv and the location (or time) of the maneuver. Included in the optimization process are the constraints required to maintain the ARTEMIS maneuvers in the spin plane. An alternative stationkeeping strategy utilizing a global search method was briefly investigated in an effort to determine the smallest Δv maneuver that maintains the spacecraft in the vicinity of the libration point for one to two additional revolutions, but was not applied to ARTEMIS because of limited spacecraft constraint modeling.

Results of Pre-flight Stationkeeping Research

Using OCS, we began with pre-flight ARTEMIS initial conditions, and a profile was generated for three maneuver locations for the aforementioned number of revolutions. Each profile varied the maneuver location and then the number of revolutions to achieve a continuation of the trajectory further downstream. Each simulation used statistically generated navigation errors and a constant maneuver execution error of +1%. In our pre-flight analysis, a spherical navigation error of 1-km position and 1-cm/s velocity (1σ), was generated by the use of an error covariance matrix. The operational uncertainty from the Goddard Trajectory Determination System (GTDS) least squares solution was found to be below 100 meters and 0.1 cm/s. During operational support, it was difficult to separate the portion of the error due to the navigation state uncertainty before maneuver execution from the maneuver execution errors because each effect was at the limit of observability.

Table 2. Control Strategy and Selection Criteria

Strategy	Goal(s)	Advantage	Disadvantage
Orbit Continuation	Velocity (or energy) is determined to deliver s/c several revs downstream (e.g., *x*-axis velocities all slightly negative)	- Guarantees a minimal Δv to achieve orbit continuation - Several control constraints can be applied - 3-D application	- Needs accurate integration and full ephemeris modeling - Logic required in program scripts to check for departure trajectories - Optimization requires monitoring of process
Mode Analysis	Determine the cartesian direction of a maneuver to maintain the orbit	- Yields mathematically desired directions	- Depended upon navigation solutions and/or predictions data that is used in Floquet analysis and building of STMs - May not meet s/c constraints in applied ΔV direction.

Table 3 summarizes the average pre-mission Δv results for cases that applied a 1.5-revolution continuation. These results include 10 trials, with each trial defined as a 4-month stationkeeping simulation run with different realizations of the errors each time. Several obvious results emerge. First, maneuvers that are applied only once per revolution are approximately an order of magnitude larger than those applied at least twice per revolution. The maneuvers applied at the maximum *y*-axis amplitude are also larger than those at the *x*-axis crossings, a result that is consistent with preliminary results from general stationkeeping analysis. To compare the results to a strategy that employs more frequent maneuvers, a scenario was simulated that applied maneuvers once every 3.8 days (i.e., a four-maneuvers-per-revolution sequence). A scenario using maneuvers at the *x*-*z* plane crossing was selected based on the operational planning considerations that ARTEMIS tracking coverage and navigation solutions would be based on a three-day arc. Interestingly, it was found that maneuvers near maximum *y*-amplitude also change the *z*-amplitude due to a jump onto a nearby quasi-halo orbit as the attitude of the spacecraft results in a *z*-axis Δv component. The pre-flight research show that maneuvers at a frequency of at least once every seven days are desired to both minimize the Δv budget and to align with the navigation solution deliveries. A more frequent maneuver plan (3.8-day updates) is only slightly better in terms of Δv. Note that these maneuver are restricted to the spin plane of the ARTEMIS spacecraft which has a spin axis aligned with the south Ecliptic pole. The maneuvers are approximately in the Ecliptic plane.

Table 3. Pre-Mission Continuous Method using 1.5-rev (10 Trials)*

Maneuver Location	No. of Maneuvers	Average Δv per Maneuver (m/s)	Std Dev (m/s)	Average Δv per Year (m/s)	Time Between Maneuver (days)
***x*-*z* plane crossing**	**15**	**0.28**	**0.78**	**12.27**	**7.3**
***x*-*z* plane crossing, once per orbit**	**7**	**4.88**	**7.07**	**106.51**	**15.2**
Max *y*-Amp Every crossing	**15**	**0.42**	**.95**	**18.13**	**7.3**
Max *y*-Amp Once per orbit	**7**	**5.46**	**6.98**	**110.91**	**14.9**
4 Pts/Rev (~3.8 days)	**33**	**0.15**	**0.33**	**13.72**	**3.8**

OPERATIONAL STATIONKEEPING OF EARTH-MOON ORBITERS

ARTEMIS Stationkeeping

The targets used for the OCS method differed slightly between the EM L_2 orbit and the EM L_1 orbit. The continuation targets for the P1spacecraft maintenance, while in orbit about EM L_2, used two different *x*-axis velocity targets, depending on which side of the orbit P1 was on. For example, targets on the far side (away from the Moon) used an *x*-axis crossing velocity of -20 m/s with a tolerance of 1 cm/s. Targets on the close side (nearer to the Moon) used *x*-axis crossing velocity targets of +10 m/s with a tolerance of 1 cm/s. Once in orbit about the EM L_1 orbit the P1 targets were changed to meet the ongoing operations similar to P2. These targets are +/- 10 cm/s at each crossing, a much smaller velocity target. The scheme here is to continuously target the next crossing downstream, up to four crossings were used as the change in the Δv after the third crossing was usually below 0.01 cm/s and therefore unachievable by the spacecraft propulsion system. As each crossing condition was achieved in the continuation process using multiple crossing targets, the Δv decreased to attain the next crossing. Also depending on the location of the maneuver with respect to the Moon radius, the Δv magnitude also varied from maneuver to maneuver.

Observed Stationkeeping Maneuver Results

Tables 4 and 5 present all the stationkeeping maneuvers for P1 and P2. The tables provide the stationkeeping number, the day of year (DOY) of the maneuver, the Δv magnitude, the cumulated Δv, the days in the libration orbit and the annual cost based on the Δv and the duration. Note that maneuver 15 for P1 was an insertion Δv during the libration transfer and is not including in the stationkeeping Δv summary.

Figures 9 through 14 summarize the chronological Δv as each stationkeeping maneuver was executed for both P1 and P2. Figures 9, 10, and 11 show the P1 Δv for each maneuver; the annual maintenance cost for P1 in L_2 and the annual cost for P1 in the L_1 orbit. Likewise, Figures 12, 13, and 14 plot the P2 Δv's for each maneuver; the annual maintenance cost for P2 in L_1 and the annual cost for P2 in the L_1 orbit when optimal planning conditions are used. For both spacecraft, the general decrease in the stationkeeping Δvs is attributed to a change in the way the spacecraft was configured to model the thrust arc over which the propulsion system was operating improvement in the modeling of the environment, and the *Cr* use from navigation solutions. Originally the thrust arc was fixed at 60 degrees. Advanced onboard software permitted this arc to be controlled (varied) more precisely and therefore the maneuver execution was more accurate. Also, the navigation solutions provided not only the state, but also a *Cr* value that considered the perturbation from solar radiation pressure. While P1 used the *Cr* provided by the navigation solution, the P2 maneuvers were originally planned with a constant *Cr* taken from pre-libration orbit analysis to determine this value. Also the peaks are attributed to the predictions of the spin axis attitude which is accurate to only approximately 1 degree. Depending on all these values, the accuracy of the maneuver varies, and therefore, the subsequent maneuver to correct any errors in addition to the general continuation of the orbit could be increased.

Stationkeeping cost since insertion into libration orbits (w/o axial corrections to extend mission three months) gives:

- Total P1 ~ 3.99 m/s
- Total P2 ~ 3.24 m/s
- P1 projected yearly stationkeeping cost ~7.39 m/s per year for L_2 and 5.28 m/s per year for L_1
- P2 projected yearly stationkeeping cost ~5.09 m/s per year
- These Δvs per year are based on ARTEMIS maneuvers schedules and constraints

Table 4. ARTEMIS P1 Stationkeeping Information

4a. P1 Individual Maneuvers

SKM	Year	DOY	Day	dv (cm/s)	cum (m/s)	Liss days	annual cost (m/s/yr)
1	2010	237	Wed	256.24		0	
2	2010	251	Wed	58.40	0.58	14	15.23
3	2010	265	Wed	22.28	0.81	28	10.52
4	2010	273	Thu	34.05	1.15	36	11.63
5	2010	282	Sat	7.96	1.23	45	9.95
6	2010	291	Mon	15.84	1.39	54	9.36
7	2010	298	Mon	11.29	1.50	61	8.96
8	2010	306	Tue	11.64	1.61	69	8.54
9	2010	313	Tue	6.96	1.68	76	8.09
10	2010	321	Wed	7.13	1.76	84	7.63
11	2010	334	Tue	20.74	1.96	97	7.39
12	2010	344	Fri	22.64	2.19	107	7.47
13	2010	352	Sat	13.79	2.33	115	7.39
14	2010	361	Mon	11.57	2.44	124	7.19
15	2011	6	Mon	3.32	2.48	134	
16	2011	17	Mon	11.80	2.59	145	6.53
17	2011	24	Mon	6.38	2.66	152	6.38
18	2011	32	Tue	19.10	2.85	160	6.50
19	2011	38	Mon	22.29	3.07	166	6.75
20	2011	45	Mon	10.30	3.17	173	6.70
21	2011	49	Fri	1.17	3.19	177	6.57
22	2011	56	Fri	5.93	3.25	184	6.44
23	2011	63	Fri	1.76	3.26	191	6.24
24	2011	69	Thu	2.93	3.29	197	6.10
25	2011	76	Thu	1.74	3.31	204	5.92
26	2011	83	Thu	2.32	3.33	211	5.77
27	2011	89	Wed	2.04	3.35	217	5.64
28	2011	96	Wed	1.99	3.37	224	5.50
29	2011	103	Wed	2.17	3.40	231	5.36
30	2011	110	Wed	27.90	3.67	238	5.63
31	2011	117	Wed	2.78	3.70	245	5.52
32	2011	124	Wed	12.99	3.83	252	5.55
33	2011	131	Wed	5.03	3.88	259	5.47
34	2011	144	Tue	5.53	3.94	272	5.28
35	2011	150	Mon	1.17	3.95	278	5.19
36	2011	157	Tue	4.03	3.99	285	5.11

4b. P2 Individual Maneuvers

SKM	Year	DOY	Day	dv (cm/s)	cum (m/s)	Liss days	annual cost (m/s/yr)
1	2010	293	Wed	11.69		0	
2	2010	300	Wed	18.38	0.18	7	9.58
3	2010	307	Wed	37.89	0.56	14	14.67
4	2010	315	Thu	24.69	0.81	22	13.43
5	2010	322	Thu	6.23	0.87	29	10.97
6	2010	333	Mon	34.85	1.22	40	11.14
7	2010	340	Mon	10.39	1.32	47	10.28
8	2010	348	Tue	6.64	1.39	55	9.23
9	2010	355	Tue	3.69	1.43	62	8.40
10	2010	362	Tue	12.13	1.55	69	8.19
11	2011	4	Tue	2.04	1.57	76	7.54
12	2011	11	Tue	11.55	1.68	83	7.41
13	2011	18	Tue	2.61	1.71	90	6.94
14	2011	25	Tue	17.85	1.89	97	7.11
15	2011	32	Tue	3.75	1.93	104	6.76
16	2011	40	Wed	29.61	2.22	112	7.24
17	2011	50	Sat	17.40	2.40	122	7.17
18	2011	56	Fri	3.63	2.43	128	6.94
19	2011	65	Sun	21.68	2.65	137	7.06
20	2011	72	Sun	20.80	2.86	144	7.24
21	2011	79	Sun	4.38	2.90	151	7.01
22	2011	86	Sun	1.99	2.92	158	6.75
23	2011	100	Sun	4.96	2.97	172	6.31
24	2011	107	Sun	4.53	3.02	179	6.15
25	2011	116	Tue	1.33	3.03	188	5.88
26	2011	123	Tue	6.85	3.10	195	5.80
27	2011	130	Tue	2.35	3.12	202	5.64
28	2011	137	Tue	1.91	3.14	209	5.49
29	2011	144	Tue	1.45	3.16	216	5.33
30	2011	152	Wed	2.43	3.18	224	5.18
31	2011	161	Mon	6.78	3.25	233	5.09

Table 5. P1 and P2 Stationkeeping Statistics

	P1 @ L_2 (cm/s)	P1 @ L_1 (cm/s)	P2 @ L_1 (cm/s)
Total Δv	**244.0**	**155.0**	**324.0**
Min Δv	**6.96**	**1.17**	**1.33**
Max Δv	**22.64**	**27.90**	**37.89**
Mean Δv	**13.51**	**7.21**	**10.85**
STD	**5.44**	**7.60**	**10.31**

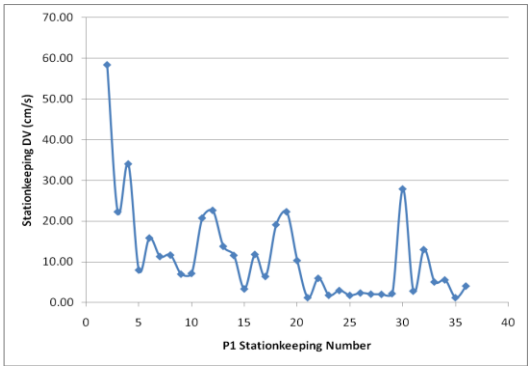

Figure 9. P1 Individual Stationkeeping Δv vs. Stationkeeping Maneuver

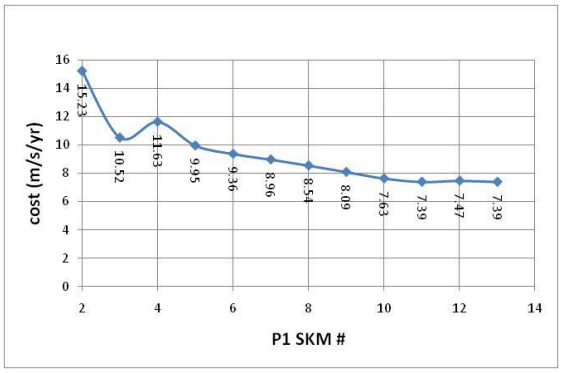

Figure 10. P1 EM L_2 Libration Point Orbit Cumulative Annual Δv

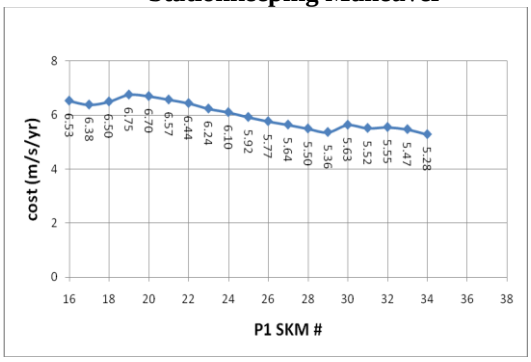

Figure 11. P1 EM L_1 Libration Point Orbit Cumulative Annual Δv

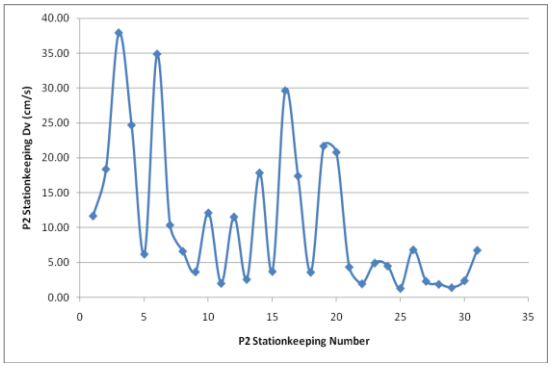

Figure 12. P2 Individual Stationkeeping Δv vs. Stationkeeping Maneuver

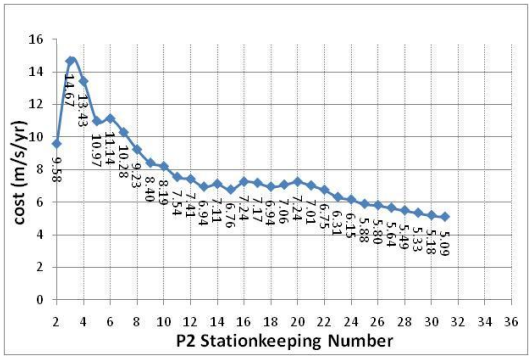

Figure 13. P2 EM L_1 Libration Point Orbit Cumulative Annual Δv (Pre Cr change)

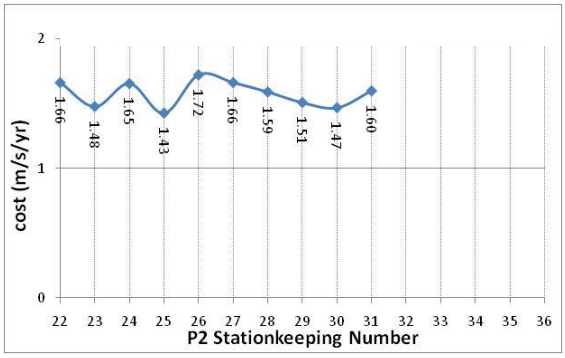

Figure 14. P2 EM L_1 Libration Point Orbit Cumulative Annual Δv (Post Cr change)

OPERATIONAL LIBRATION FLOQUET MODE RESULTS

Research involving multi-body environments has been ongoing for over a decade.[20-22,27] Working in collaboration with Purdue University, GSFC analyzed many trajectories in both Sun-Earth and Earth-Moon regimes. This analysis has demonstrated that there could be alternate methods for stationkeeping that result in the balancing or continuation of the libration orbit over several revolutions. In general terms, this research is denoted here as Mode Analysis and analyzes the eigenstructure (eigenvectors and eigenvalues) of the libration orbit to compute information regarding the orbit stability. By proper modeling of the orbit using various methods such as CR3B and geometric means, many studies have been completed that indicate that maneuvers along the stable or unstable mode direction, as represented in a Cartesian system, could be used for

stationkeeping. ARTEMIS permits us to validate that research and show how the OCS used for ARTEMIS placed maneuvers along the stable mode direction.

Using operational ARTEMIS orbit determination solutions along with the stationkeeping maneuvers executed using the OCS strategy, we computed an approximate monodromy matrix by generating and propagating the State Transition Matrix (STM), Φ, from an initial state. To calculate the STM, we propagate an initial state that is perturbed in each of its components (4×10^{-4} km and 1×10^{-4} cm/s for each position and velocity). Then, in Matlab, a finite-difference STM using initial and final state information from numerical integration yields an approximation of the monodromy matrix.

$$\frac{d}{dt}\Phi(t,t_0) = A(t)\Phi(t,t_0) \text{ and } \Phi(t,t_0) = \frac{\delta X_{t1}}{\delta X_{t0}} = \begin{bmatrix} \frac{\delta r_{t1}}{\delta r_{t0}} & \frac{\delta r_{t1}}{\delta v_{t0}} \\ \frac{\delta v_{t1}}{\delta r_{t0}} & \frac{\delta v_{t1}}{\delta v_{t0}} \end{bmatrix} \tag{3}$$

From this information, we then compute the 6 eigenvalues, λ_i, of the STM which yields,

- $|\lambda_i| < 1 \rightarrow$ stable eigenvalue(s)
- $|\lambda_i| > 1 \rightarrow$ unstable eigenvalue(s)

Once the mode information is generated we compare actual maneuver direction with stable/unstable eigenvector information. Additional methods are being studied for computing eigenvalues/eigenvectors in less periodic portions of the orbits (i.e., the P1 L_2 quasi-halo trajectory).

Below are three figures (Figures 15, 16, and 17) that reflect the stable and unstable mode directions for ARTEMIS orbits consistent with P1 over one revolution of an EM L_2 orbit, P1 in an EM L_1 revolution and P2 as it evolves over a revolution about the EM L_1 point. Additionally, several plots present information for a

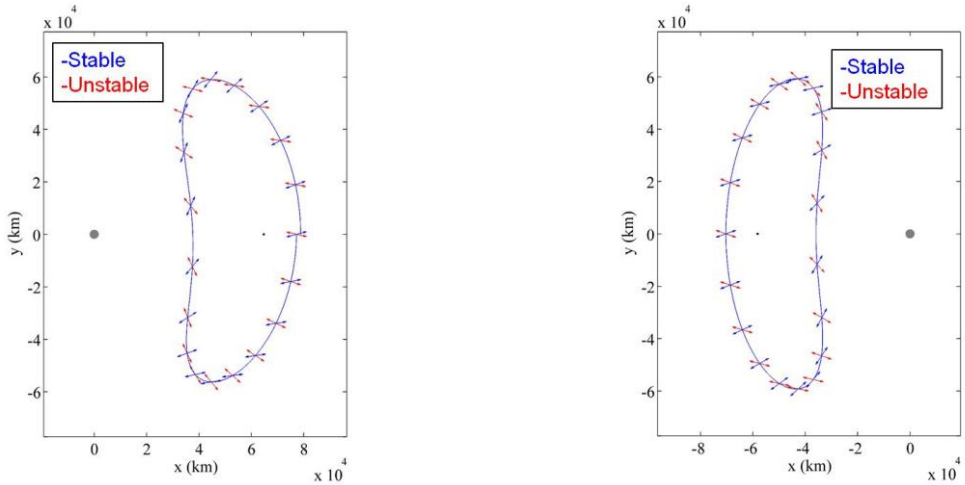

Figure 15. P1 EM L_2 (right) and EM L_1 (left) Stable and Unstable Directions

select few stationkeeping maneuvers. Note that all the ARTEMIS maneuvers are co-aligned along the stable mode direction. Analysis was also performed to determine if a Δv along the unstable direction would maintain the orbit. This proved valid, but the OCS optimization scheme and the stable mode direction results in minimal Δv magnitudes which were smaller that the unstable component by ~5-10%. Initially, it may be surprising that all the Δvs are aligned with the stable mode rather than the unstable mode to cancel that unstable component of the error. At this point, we believe that the OCS process employs the selected targets to 'bend' the trajectory

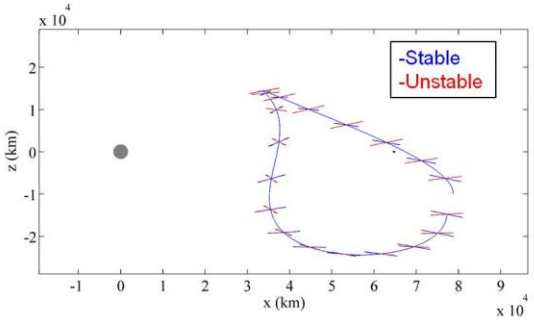

Figure 16. Sample P1 EM L_2 (side view)

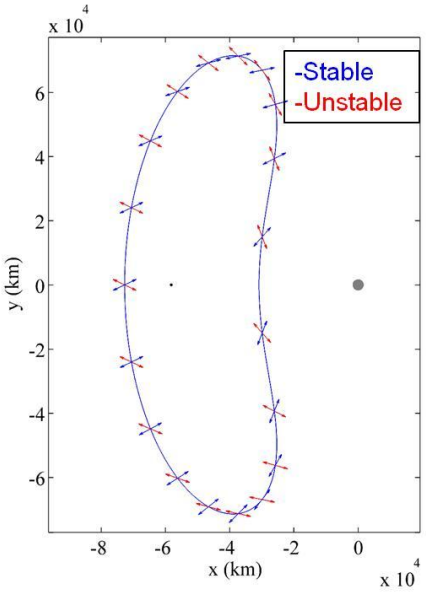

Figure 17. P2 EM L_1 Stable and Unstable Directions

along a continuation orbit that, in fact, results in a maneuver that promotes the stability of the orbit; in contrast to an action that reduces the unstable component. We also believe that the use of multiple orbits in our optimization algorithm aids in delivering maneuvers in the stable direction. While a full understanding of this is still being examined, a basic conclusion is that maneuver placement along the stable mode can be used to maintain the orbit.

In Figures 18 and 19, the stationkeeping Δv directions and the stable / unstable mode directions at these maneuver epochs (location) are plotted. Figures 20 and 21 present the angle between the EM rotating coordinate system Cartesian Δv vector and the stable mode directions for all stationkeeping maneuvers. As apparent in these figures, the Δv vector aligns closely with the stable mode for all maneuvers even with spacecraft constraints in place.

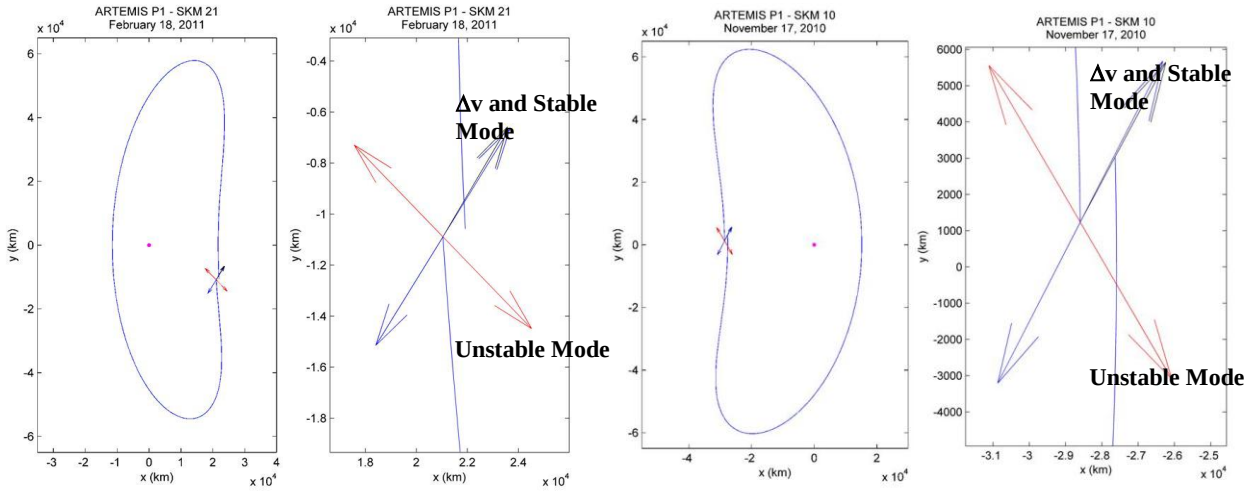

Figure 18. P1 Stationkeeping #21 (left) and Stationkeeping #10 (right) Locations, Stable (blue) and Unstable (red) Directions and the Δv (black) Direction

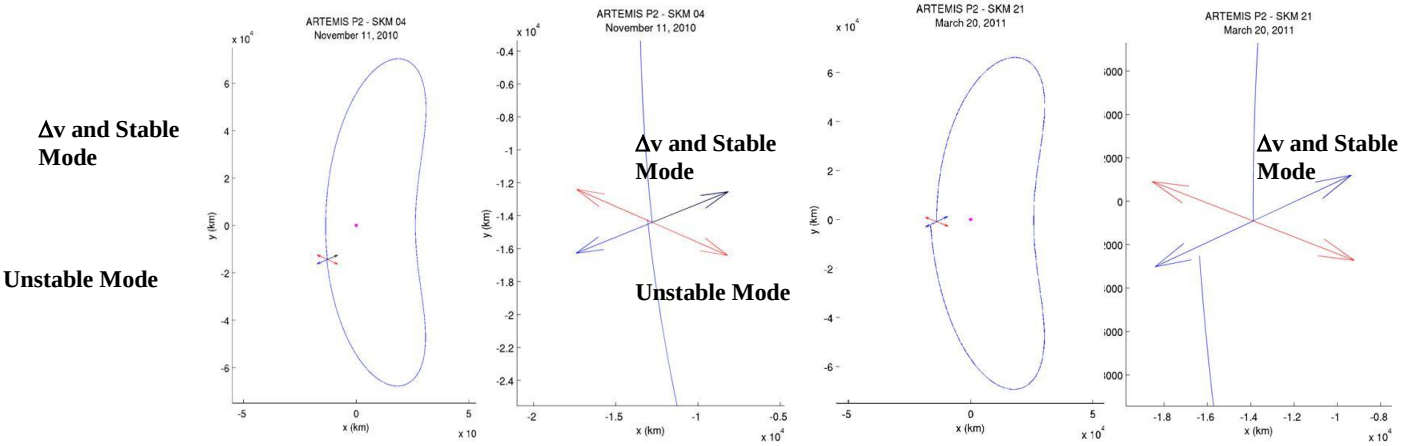

Figure 19. P2 SKM 04 (left) and SKM 21 (right) Locations, Stable (blue) and Unstable (red) Directions and the Δv (black) Direction

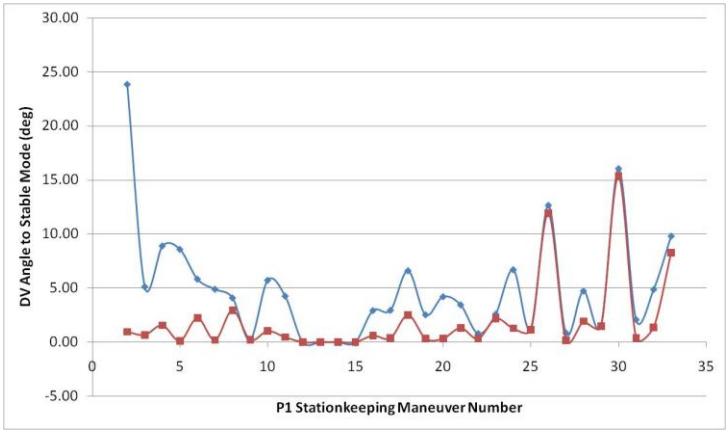

Figure 20. P1 Total (top, blue) and In-Plane (bottom, red) Angle between Δv Vector and the Associated Stable Mode Direction

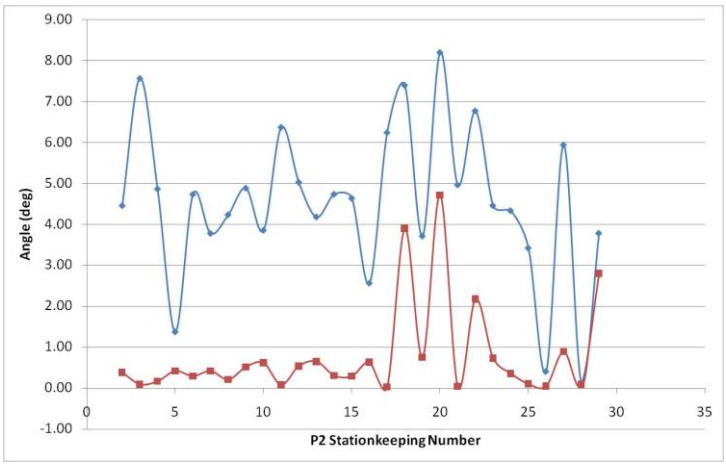

Figure 21. P2 Total (top, blue) and In-Plane (bottom, red) Angle between Δv Vector and the Associated Stable Mode Direction

Observations and Recommendations

Research and demonstrated operations have provided some unique observations for the selection of Earth-Moon libration orbits and their stationkeeping. It has been demonstrated that low stationkeeping Δvs can be found to meet mission requirements.

- **Modeling and Poincare Maps**
  - A CR3B model can be used to estimate non-linear Earth-Moon libration orbits to a reasonable level of fidelity, especially when combined with navigation solutions.
  - Earth-Moon Poincaré Maps provide accurate details of the dynamics. They also provide a guide for orbit characteristics selection and initial maneuver locations.
  - To first order, the dynamics of the Earth-Moon environment also must be modeled over a sufficient duration of 21 days to realistically account for all accelerations.
  - A full ephemeris model and the modeling of associated errors from navigation and maneuvers are required to accurately determine the accelerations that affect the stationkeeping Δv.
- **Stationkeeping and Control**
  - Optimized maneuver directions were aligned with the dynamically stable mode direction for all stationkeeping maneuvers.
  - Stationkeeping cost with realistically modeled navigation errors does have a floor – a rule of thumb from the ARTEMIS mission was a ~20:1 ratio of SKM Δv to navigation + execution errors for a ½ revolution.
  - Targeting goals used for EM L_2 stationkeeping differed from EM L_1 stationkeeping goals.
  - Maneuvers performed at the *y*-extrema resulted in an increased 'unstableness' of the orbit resulting in increased Δv magnitudes for follow-on maneuvers.
  - The OCS stationkeeping strategy can meet rigorous mission requirements and provides a robust method that can be verified with Mode Analysis.

An operational note, two other items of interest also were observed during the ARTEMIS mission support; sensitivity of the post-maneuver orbit with respect to maneuvers located at the *x*-z plane crossing or *y*-extreme and the effect of the lunar eccentricity to reduce the libration orbit negative *y*-amplitude every two weeks. Due to station contact schedule, some stationkeeping maneuvers were placed near the *y*-component extreme. We found that the resultant follow-up stationkeeping maneuver was larger, almost a factor of 5 times larger than expected. Subsequent analysis found that the Δv directions were co-aligned with the spacecraft velocity vector direction at these locations, unlike at the *x*-axis crossing where the Δv vector was almost perpendicular. Our analysis indicates that this alignment results in more uncertainty in the final velocity after the Δv was applied. We then switched back to *x*-z plane crossing locations when the station contact permitted. Consideration of errors in the onboard computation of the center of the spin pulse (Δv direction) contributed to this sensitivity as well.

SUMMARY

An Earth-Moon orbit selection process using Poincaré maps and a stationkeeping strategy has been demonstrated that results in low stationkeeping Δv requirements which met the ARTEMIS mission requirements and spacecraft constraints. It has been demonstrated that a full ephemeris model along with accelerations from third-body perturbations and the Earth's potential must be modeled for accurate prediction and maneuver planning. Associated errors from navigation and maneuvers must be kept to levels below tenths of cm/s to accurately model the accelerations that affect the Δv. The dynamics of the Earth-Moon environment also must be modeled over a sufficient duration, at least 3 weeks. This duration should be equal to or greater than 21 days to account for the lunar eccentricity and to a lesser, but still important degree, the perturbation from the Sun. An increase in the frequency of the maneuvers tends to reduce the overall Δv requirements as does the placement of the maneuvers near the *x*-z plane crossing. Operational ARTEMIS stationkeeping costs had a floor of about 5 m/s per year, considerably less than previous studies.

CONCLUSIONS

While there are a number of strategies available that incorporate the Earth-Moon dynamics, the actual mission applications and mission constraints must also be considered. The methods here provide a general stationkeeping algorithm that is capable of meeting spacecraft constraints on Δv direction or additional orbit parameters and does not require a reference trajectory. The required stationkeeping Δv can be minimized and has been demonstrated to be very minimal at ~5 m/s per year. With the ARTEMIS P1 and P2 Earth-Moon libration point orbit completed, investigation of additional robust strategies and options to improve the Δv computation for stationkeeping is continuing.

REFERENCES

1. D. Folta, M. Woodard, and D. Cosgrove, "Stationkeeping of the First Earth-Moon Libration Orbiters: the ARTEMIS Mission," *AAS/AIAA Astrodynamics Specialist Conference*, Girdwood, Alaska, July 31-August 4, 2011. Paper No. AAS 11-515.
2. D. Folta, T. Pavlak, K. Howell, M. Woodard, D. Woodfork, "Stationkeeping of Lissajous Trajectories in the Earth-Moon System with Applications to ARTEMIS," *20th AAS/AIAA Space Flight Mechanics Meeting*, San Diego, California, February 14-17, 2010. Paper No. AAS 10-113.
3. M. Woodard, D. Folta, and D. Woodfork, "ARTEMIS: The First Mission to the Lunar Libration Points," *21st International Symposium on Space Flight Dynamics*, Toulouse, France, September 28-October 2, 2009.
4. D. Folta, M. Woodard, K. Howell, C. Patterson, and W. Schlei, "Applications of Multi-Body Dynamical Environments: The ARTEMIS Transfer Trajectory Design", *Acta Astronautica*,Vol. 73, 2012, pp. 237–249.
5. Sibeck, D.G., et al. (2011), ARTEMIS Science Objectives and Mission Phases, Space Sci. Rev., doi: 10.1007/s11214-011-9777-9. http://www.springerlink.com/content/p615274351124111/fulltext.pdf
6. V. Szebehely, *Theory of Orbits: The Restricted Problem of Three Bodies*. Academic Press Inc., New York, 1967.
7. C. Conley, "Low Energy Transit Orbits in the Restricted Three-Body Problem," *Society for Industrial and Applied Mathematics Journal on Applied Mathematics*, Vol. 16, 1968, pp. 732-746.
8. W. Koon, M. Lo, J. Marsden, and S. Ross, "Heteroclinic Connections between Periodic Orbits and Resonance Transitions in Celestial Mechanics," *Chaos*, Vol. 10, June 2000, pp. 427-469.
9. G. Gómez, W. Koon, M. Lo, J. Marsden, J. Masdemont, and S. Ross, "Connecting Orbits and Invariant Manifolds in the Spatial Restricted Three-Body Problem," *Nonlinearity*, Vol. 17, September 2004, pp. 1571-1606.
10. K. Howell, "Families of Orbits in the Vicinity of the Collinear Libration Points," *Journal of the Astronautical Sciences*, Vol. 49, No. 1, January-March 2001, pp. 107-125.
11. R. Farquhar and A. Kamel, "Quasi-Periodic Orbits about the Translunar Libration Point," *Celestial Mechanics*, Vol. 7, 1973, pp. 458-473.
12. D. Richardson and N. Cary, "A Uniformly Valid Solution for Motion about the Interior Libration Point of the Perturbed Elliptic-Restricted Problem," *Astrodynamics Specialist Conference*, Nassau, Bahamas, July 28-30, 1975. Paper No. AAS 75-021.
13. K. Howell, and H. Pernicka, "Numerical Determination of Lissajous Trajectories in the Restricted Three-Body Problem," *Celestial Mechanics*, Vol. 41, Nos. 1-4, 1988, pp. 107-124.
14. E. Kolemen, J. Kasdin, and P. Gurfil, "Quasi-Periodic Orbits of the Restricted Three-Body Problem Made Easy", *New Trends in Astrodynamics and Applications III, AIP Conference Proceedings*, Vol. 886, pp. 68-77, Princeton, New Jersey, August 16-18, 2007.
15. D. Grebow, "Generating Periodic Orbits in the Circular Restricted Three-Body Problem with Applications to Lunar South Pole Coverage." M.S. Thesis, School of Aeronautics and Astronautics, Purdue University, West Lafayette, Indiana, 2006.
16. G. Gómez, À. Jorba, J. Masdemont, C. and Simó, *Dynamics and Mission Design Near Libration Points, Vol. III: Advanced Methods for Collinear Points*. River Edge, NJ: World Scientific Publishing Co., 2001.
17. B. Barden and K. Howell, "Fundamental Motions Near Collinear Libration Points and Their Transitions," *Journal of the Astronautical Sciences*, Vol. 46, No. 4, October-December 1998, pp. 361-378.
18. D. Hoffman, "Stationkeeping at the Collinear Equilibrium Points of the Earth-Moon System," NASA JSC-26189, September 1993.
19. R. Farquhar, "The Utilization of Halo Orbits in Advanced Lunar Operation," NASA TN D-6365, GSFC, Greenbelt, Maryland, 1971.
20. C. Renault and D. Scheeres, "Statistical Analysis of Control Maneuvers in Unstable Orbital Environments," *Journal of Guidance, Control, and Dynamics*, Vol. 26, No. 5, September-October 2003, pp 758-769.

21. K. Howell and T. Keeter, "Station-Keeping Strategies for Libration Point Orbits: Target Point and Floquet Mode Approaches," *Proceedings of the AAS/AIAA Spaceflight Mechanics Conference 1995*, Advances in the Astronautical Sciences, Vol. 89, R. Proulx, J. Liu, P. Seidelmann, and S. Alfano (editors), 1995, pp. 1377-1396.
22. G. Gómez, J. Llibre, R. Martínez, and C. Simó, *Dynamics and Mission Design Near Libration Points, Vol. I: Fundamentals: The Case of Collinear Libration Points*, World Scientific Monograph Series, World Scientific Publishing Ltd., Singapore, 2001.
23. B. Marchand, and K. Howell, "Formation Flight Near L1 and L2 in the Sun-Earth-Moon Ephemeris System Including Solar Radiation Pressure," *AAS/AIAA Astrodynamics Specialist Conference*, Big Sky Montana, August 2003. Paper No. AAS 03-596.
24. D. Folta, and F. Vaughn, "A Survey of Earth-Moon Libration Orbits: Stationkeeping Strategies and Intra-Orbit Transfers," *AIAA/AAS Astrodynamics Conference*, Providence, Rhode Island, August 2004. AIAA Paper No. 2004-4741.
25. T. Pavlak and K. Howell, "Strategy for Long-Term Libration Point Orbit Stationkeeping in the Earth-Moon System," *AAS/AIAA Astrodynamics Specialist Conference*, Girdwood, Alaska, July 31-August 4, 2011.
26. K. Williams, B. Barden, K. Howell, M. Lo, and R. Wilson, "GENESIS Halo Orbit Stationkeeping Design," *International Symposium: Spaceflight Dynamics*, Biarritz, France, June 2000.
27. K. Howell, and H. Pernicka, "Station-Keeping Method for Libration Point Trajectories," *Journal of Guidance, Control, and Dynamics*, Vol. 16, No. 1, January-February 1993, pp. 151-159.